



# A Two Level Control Algorithm for the Maximum Power Point Tracking of Solar Photovoltaic System

Sneha V L<sup>1</sup>, Revathy Sasidharan<sup>2</sup>

PG Student, Electrical and Electronics Dept., Lourdes Matha College of Science & Technology Trivandrum, India<sup>1</sup>

Asst Professor, Electrical and Electronics Dept., Lourdes Matha College of Science & Technology Trivandrum, India<sup>2</sup>

**Abstract:** Solar photovoltaic (PV) energy has witnessed double digit growth in the past decade. Maximum power point tracking algorithm (MPPT) keeps the photovoltaic systems continuously delivering the maximum power output to the utility, regardless of the variation in environment condition. To improve the performance of MPPT, a two-level adaptive control architecture is proposed here. System complexity is reduced, control and the uncertainties in the photovoltaic systems are effectively handled. The first level of control is ripple correlation control (RCC) which is an MPPT method copes with many drawbacks of other algorithms and the second level of control is model reference adaptive control (MRAC) which compensates for the undesired characteristic of the photovoltaic power conversion system. By coupling these two control algorithms, the system achieves MPPT with overall system stability. From the results, the proposed control algorithm enables the system to converge to the maximum power point in milliseconds. The system shows no oscillatory response even after there is a change in the environmental conditions.

**Keywords:** Maximum power point tracking (MPPT), Photovoltaic system, Ripple correlation control (RCC), Model reference adaptive controller (MRAC)

## I. INTRODUCTION

RECENTLY, there has been significant environmental and political motivation to shift domestic power generation to renewable sources such as wind and solar. Solar power is at the forefront of clean, renewable energy, and it is gaining momentum due to advances in solar panel manufacturing and efficiency as well as increasingly volatile fuel costs. Solar power is an attractive option because of the large amount of power available in incident sunlight, particularly in large industrial parks and residential suburbs. Photovoltaic system is a critical component to achieve the solar energy through an environmentally-friendly and efficient way. However, photovoltaic (PV) solar cells, the most readily available solar technology, operate best on bright days with little or no obstruction to incident sunlight.

The operating current and voltage of solar panels, which maximize power output are dependent on environmental conditions. In order to maintain efficient operation despite environmental variations, one approach is to use a maximum power point tracking (MPPT) algorithm to dynamically tune either control current or voltage to the maximum power operating point. Maximum power point tracking algorithm (MPPT) keeps the photovoltaic systems continuously delivering the maximum power output to the utility, regardless of the variation in environment condition. Under the effect of MPPT algorithm, the photovoltaic systems are capable of adapting itself to the environment change and delivering the maximum power

output. Generally, the MPPT controller is embedded in the power electronic converter systems, so that the corresponding optimal duty cycle is updated to the photovoltaic power conversion system to generate the maximum power point output [1],[2].

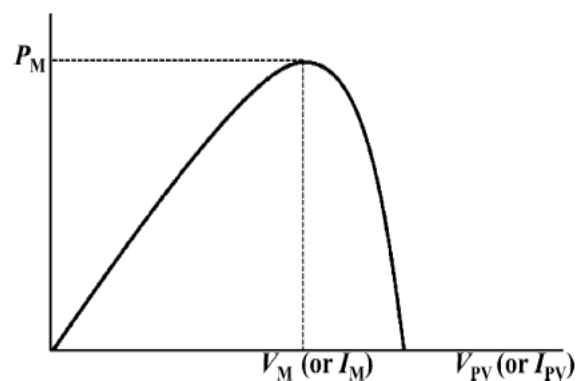


Fig. 1. Power-voltage characteristics of photovoltaic systems

Several MPPT algorithms have been reported in the past few decades. The P&O MPPT algorithm is mostly used, due to its ease of implementation. It is based on the following criterion: if the operating voltage of the PV array is perturbed in a given direction and if the power drawn from the PV array increases, this means that the operating point has moved toward the MPP and, therefore,



the operating voltage must be further perturbed in the same direction. Otherwise, if the power drawn from the PV array decreases, the operating point has moved away from the MPP and, therefore, the direction of the operating voltage perturbation must be reversed. Drawback of P&O MPPT technique is that, at steady state, the operating point oscillates around the MPP giving rise to the waste of some amount of available energy. Several improvements of the P&O algorithm have been proposed in order to reduce the number oscillations around the MPP in steady state, but they slow down the speed of response of the algorithm to changing atmospheric conditions and lower the algorithm efficiency during cloudy days [6]. The incremental conductance (INC) method uses the fact that the derivative of the array power with respect to the array voltage is ideally zero at the MPP (see Fig.1), positive to the left of the MPP, and negative to the right of the MPP. The INC method has been shown to perform well under rapidly changing environmental conditions, but at the expense of increased response times due to complex hardware and software requirements. Besides the P&O and the INC algorithms, there are many other advanced algorithms have been addressed, such as fuzzy logic and the neural network-based algorithms [8-10]. These methods are suitable for solving certain specific problems; however, the realization of the system is overwhelmingly complex in the software and hardware construction of the solar panel. To this end, a general problem associated with MPPT algorithms is the transient oscillations in the system's output voltage after the duty cycle is rapidly changed in order to track the MPP [7].

Thus, an ideal MPPT control algorithm would be simple inexpensive, and would show a rapid convergence to the MPP with minimal oscillation in the output voltage. A two-level MPPT control algorithm that consists of ripple correlation control (RCC) [11]–[14] in the first level and model reference adaptive control (MRAC) [15], [16] in the second level is proposed (see fig 2). In the first control level the array voltage and power serve as the inputs to the RCC unit. The RCC unit then calculates the duty cycle of the system,  $d(t)$ , to deliver the maximum available power to the load in the steady state. In the second control level, the new duty cycle calculated from the RCC unit is routed into an MRAC architecture, where the dynamics of the entire photovoltaic power conversion system, or the plant, are improved to eliminate any potential transient oscillations in the system's output voltage. Transient oscillations in the system's output voltage can result after the duty cycle has been updated to account for rapidly changing atmospheric conditions. To prevent the plant from displaying such oscillations, a critically damped system is implemented as the reference model. During adaptation, the error between the plant and reference model is utilized to tune the parameters in the controller. Properly tuning the controller parameters enables the output of the plant to match the output of the reference model, at which point the error converges to zero and the maximum power is obtained.

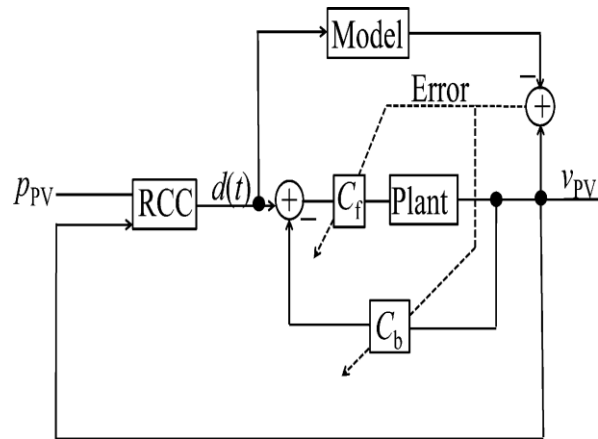


Fig. 2. Proposed MPPT control architecture

II. SYSTEM DESCRIPTION

A. PV modelling

A solar panel cell basically is a p-n semiconductor junction when exposed to the light, a DC current is generated. The generated current varies linearly with the solar irradiance [14]. The equivalent electrical circuit of an ideal solar cell can be treated as a current source parallel with a diode shown in figure 3.

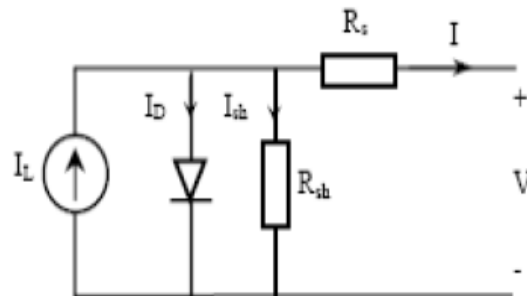


Fig. 3: Equivalent electrical circuit of a solar cell

The solar cell output current is given by,

$$I = I_L - I_D - I_{Sh} \tag{1}$$

The current through diode is given by,

$$I_D = I_0 \left\{ \exp \left[ \frac{q(V + IR_s)}{AKT_C} \right] - 1 \right\} \tag{2}$$

Therefore (1) becomes

$$I = I_L - I_0 \left\{ \exp \left[ \frac{q(V + IR_s)}{AKT_C} \right] - 1 \right\} - \frac{V + IR_s}{R_{Sh}} \tag{3}$$

B. PV characteristics

Photovoltaic system can regulate the voltage or current of the solar panel using a dc–dc converter interfaced with an MPPT controller to deliver the maximum allowable power [17], [18]. Fig. 4 shows the integration of such a system



where a boost converter is utilized to deliver optimal power to the load. In the boost converter system shown in Fig. 4, the MPPT controller senses the voltage and current of the solar panel and yields the duty cycle  $d$  to the switching transistor  $S$ . The duty cycle of the transistor is related to the array voltage through

$$v_{PV} = i_{PV} R_0 (1 - d^2) \tag{4}$$

where  $v_{PV}$  and  $i_{PV}$  are the array voltage and current, respectively, and  $R_0$  is the load resistance. The goal then is to design a controller that continually calculates the optimal value of the duty cycle so that array voltage tracks maximum voltage and thus delivers the maximum available power.

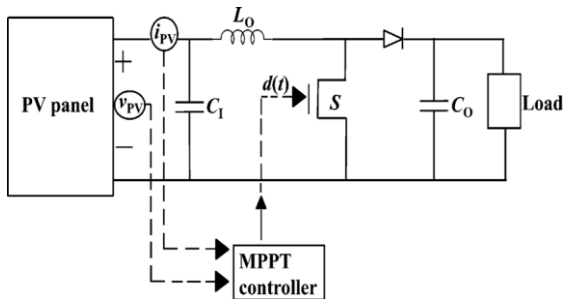


Fig. 4. MPPT controller of a photovoltaic boost converter system

### C. Dynamics of converter

The relationship (4) provides the foundation for conventional MPPT algorithms to compute the converter's duty cycle in steady states. However, to optimize transient responses, the MPPT control must consider the dynamics between the duty cycle and array voltage. Since transient oscillations are undesired and can lead to inefficient operation of the system, the MPPT control needs to eliminate transient oscillations in the array voltage after the duty cycle has been updated to account for changing environmental conditions. To simplify the analysis of the system's transient response, we consider a small signal equivalent circuit (see Fig.5) as suggested in [7]. A resistor  $R_1$  is used to model the solar array with a small signal array voltage  $v_{PV}$  and small signal array current  $i_{PV}$  across its terminals. We now derive the transfer function from the control signal (duty cycle) to the array voltage in small signal operation around an operating point. This transfer function characterizes the dynamics of the system. It should be noted that the dynamic model in Fig. 5 shows the load of the boost converter as a storage battery, which is practical for photovoltaic systems. While this representation will change the value of  $v_{PV}$  given in (1) and move the operating point in the steady-state response, it will have little effect on the system's frequency response for the range of frequencies near the natural frequency,

where we see resonances or under damped oscillations. Therefore, we ignore the dynamics of the battery in the derivation of the transfer function from the duty cycle to the array voltage in small signal operation.

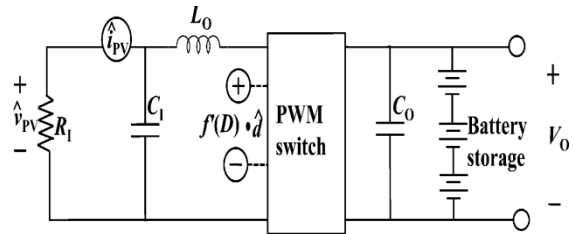


Fig. 5. Small signal equivalent circuit of photovoltaic power conversion system

In analysing Fig. 5, we have the following relationship in the frequency domain or s-domain:

$$\frac{\hat{v}_{PV}}{R_1} + s \hat{v}_{PV}(s) C_1 = \frac{f'(D) \hat{d}(s) - v_{PV}(s)}{s L_0} \tag{5}$$

Where  $s$  is the Laplace variable,  $\hat{d}$  represents the small signal variation around the converter's duty cycle  $D$  at the operating point,  $\hat{d}(s)$  and  $\hat{v}_{PV}(s)$  are the Laplace transforms of  $d(t)$  and  $v_{PV}(t)$ , respectively,  $f(D)$  is the relationship between the operating duty cycle,  $D$  and the steady-state dc input voltage of the boost converter,  $f'(D)$  is the derivative of  $f(D)$  with respect to the duty cycle at the operating point  $D$ . From (5) we obtain,

$$\frac{\hat{v}_{PV}(s)}{\hat{d}(s)} = \frac{f'(D)}{L_0 C_1 s^2 + \frac{L_0}{R_1} s + 1} \tag{6}$$

It is known that,

$$f(D) = V_{PV} = (1 - D)V_0 \tag{7}$$

where  $V_0$  is the steady-state dc output voltage of the boost converter.

From (7), we have

$$f'(D) = -V_0 \tag{8}$$

and thus (6) turns to

$$\frac{\hat{v}_{PV}(s)}{\hat{d}(s)} = \frac{-V_0}{s^2 + \frac{1}{R_1 C_1} s + \frac{1}{L_0 C_1}} \tag{9}$$

The minus sign in (9) indicates that decreasing the duty ratio will increase the panel voltage. The aforementioned



transfer function is derived from a linearized version (see Fig. 5) of the nonlinear system in Fig. 4, around a single operating point. By using the aforementioned transfer function the behaviour of system transient oscillations can be analysed.

### III. PROPOSED METHOD OF MPPT

A two level control algorithm is proposed here. In the first control level, RCC is utilized to calculate the duty cycle of the converter, to deliver maximum available power to the load in the steady state. In the second control level, an MRAC structure which regulates the dynamics of the converter in response to the duty cycle calculated from RCC, preventing the array voltage from transient oscillations after changes in solar insolation. The RCC level is responsible to handle changes in solar insolation, and the tuning process of RCC should be fast enough to catch up to the changes in solar insolation. The tuning process of MRAC must be fast enough to catch up to the changes in the operating point of the converter and the responses of RCC.

#### A. Ripple correlation control

The RCC calculates the duty cycle that delivers the maximum power to the load in the steady state. The main innovation of RCC is to use the switching ripple inherent to the converter to perturb the system and thus track the MPP [14]. The RCC is essentially an improved version of the P&O method [3]–[5] except that the perturbation is inherent to the converter. Such a methodology is advantageous because it negates the necessity for external circuitry to inject the perturbation. In addition, RCC has been proven to converge asymptotically to the MPP with minimal controller complexity and straight-forward circuit implementation [14]. The RCC is based on the observation that the product of the time-based derivatives of the array voltage and power will be greater than zero to the left of the MPP, less than zero to the right of the MPP, and exactly zero at the MPP (see Fig. 1.)

$$\frac{dp_{PV}}{dt} \frac{dv_{PV}}{dt} > 0 \text{ when } V_{PV} < V_M \quad (10)$$

$$\frac{dp_{PV}}{dt} \frac{dv_{PV}}{dt} < 0 \text{ when } V_{PV} > V_M \quad (11)$$

$$\frac{dp_{PV}}{dt} \frac{dv_{PV}}{dt} = 0 \text{ when } V_{PV} = V_M \quad (12)$$

These observations lead to the control law

$$\frac{d d(t)}{dt} = k \frac{dp_{PV}}{dt} \frac{dv_{PV}}{dt} \quad (13)$$

Where  $k$  is a constant of negative gain. The control law (13) can be qualitatively described as follows: if  $v_{PV}$  increases and there is a resulting increase in  $p_{PV}$ , the

system's operating point is to the left of the MPP (see Fig. 1) and therefore  $d$  should decrease causing an increase of  $v_{PV}$  according to (4); if  $p_{PV}$  decreases after an increase in  $v_{PV}$ , then the system's operating point is to the right of the MPP (see Fig. 1) and thus  $d$  should increase in order to reduce  $v_{PV}$ . From inspection of (12) and (13), the goal then is to drive the time-based derivative of  $d$  to zero so that maximum power is obtained. As established in [11]–[14], RCC has a well-developed theoretical basis and has been mathematically proven to yield the optimal value of the duty cycle in order to deliver maximum power in the steady state. The advantage of RCC over conventional algorithms such as P&O, is that in the steady-state RCC converges to the MPP while P&O oscillates around the MPP. Relative to fuzzy logic and neural networks, RCC is advantageous due to its simple implementation as well as its low cost. In addition to steady-state analysis, one must also consider the transient response of the boost converter system so that the controller can rapidly converge to the theoretical MPP with minimal oscillation. In the next section, an MRAC algorithm is proposed to prevent the array voltage from exhibiting an under damped response.

#### B. Proposed model reference adaptive controller

In the previous section, RCC is used to calculate the duty cycle aimed at delivering the maximum available power in the steady state. It is also desired that the system converges to the MPP swiftly during changes in solar insolation. As shown in (9), the relationship between the array voltage and the converter duty cycle is a highly dynamic process. Since the operating point will vary as solar insolation varies, it is not guaranteed that the array voltage exhibits critically damped behaviour without adaptive control. The MRAC architecture proposed here is to maintain a critically damped behaviour of the array voltage. The basic idea of MRAC is to design an adaptive controller so that the response of the controlled plant remains close to the response of a reference model with desired dynamics, despite uncertainties or variations in the plant parameters. The proposed architecture of MRAC is shown in Fig. 6. The input to the overall system,  $r(t)$ , is the change in duty cycle calculated using RCC. The plant model in Fig. 6 corresponds to the transfer function in (9). However, for convenience, we change its sign (by multiplying  $-1$  to it) so that the plant model has only positive coefficients. We use  $y_p(s)$  to represent the output of the plant and  $u_p(s)$  to represent input thus the plant model is expressed as,

$$G_p(s) = \frac{y_p(s)}{u_p(s)} = \frac{k_p(s)}{s^2 + a_p s + b_p} \quad (14)$$

where the values and meanings of  $k_p$ ,  $a_p$ , and  $b_p$  can be implied from (9). The reference model is chosen to exhibit desired output  $y_m(t)$  for input  $r(t)$





$$G_m(s) = \frac{y_m(s)}{r(s)} = \frac{k_m(s)}{s^2 + a_m s + b_m} \quad (15)$$

where  $k_m$  is a positive gain, and  $a_m$  and  $b_m$  are determined so that the reference model delivers a critically damped step response. The main control objective is to design so that tracks  $y_m(t)$ .

Controller Structure: To achieve the control objective, we use the controller structure shown in Fig. 6(b). The expression for the controller is

$$u_p = \theta_0 r + \theta_1 \frac{1}{s + \lambda} u_p + \theta_2 \frac{1}{s + \lambda} y_p + \theta_3 y_p \quad (16)$$

$$= \theta_0 r + \theta_1 \omega_1 + \theta_2 \omega_2 + \theta_3 y_p = \theta^T \omega$$

Where  $\theta = [\theta_0, \theta_1, \theta_2, \theta_3]^T$  is the parameter vector of the controller and  $\omega$  is defined as,

$$\omega = [r, \omega_1, \omega_2, y_p]^T$$

It is shown in [16] that the controller structure (16) is adequate to achieve the control objective: it is possible to make the transfer function from  $r$  to equal to  $y_m(t)$  specifically when

$$\theta = \theta^* = [\theta_0^*, \theta_1^*, \theta_2^*, \theta_3^*]^T \quad (17)$$

with,

$$\theta_0^* = \frac{k_m}{k_p}$$

$$\theta_1^* = a_p - a_m$$

$$\theta_2^* = \frac{(a_p - a_m)(-\lambda^2 + \lambda a_p - b_p)}{k_p}$$

$$\theta_3^* = \frac{b_p - b_m + (a_p - a_m)(\lambda - a_p)}{k_p} \quad (18)$$

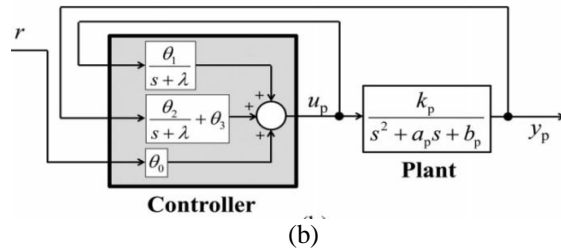
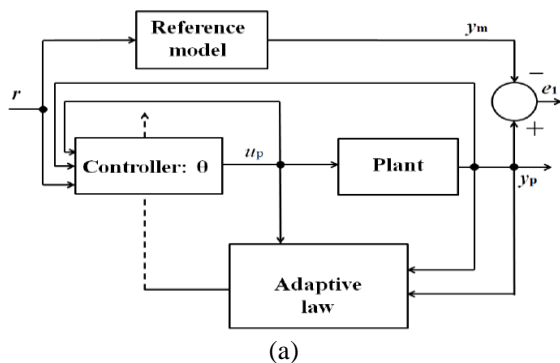


Fig. 6. (a) Proposed MRAC structure. (b) Controller structure in the proposed MRAC.

The adaptive law of the controller is

$$\dot{\theta} = -\gamma e_0 y_p \quad (19)$$

#### IV. SIMULATION RESULTS

The adaptive controller presented in Section III was then simulated for verification. The plant and controller parameters are listed in Table I. The plant model was chosen to deliver an actual array voltage with an under damped step response. The reference model was designed to deliver a theoretical MPP voltage with a critically damped step response. Its damping ratio, which equals to

$\frac{a_m}{2\sqrt{b_m}}$  is the determining factor as inferred from (15).

Normally, the ratio is chosen to be either exactly 1 or slightly less than 1. In the latter case, the step response rises faster at the cost of slight overshoot. The desired outcome of simulation would be that after the plant has undergone the adaptation phase, the parameters of the controlled plant would converge to the parameters of the reference model and thus the adapted array voltage would show critically damped behaviour.

TABLE I PARAMETERS USED FOR ADAPTIVE CONTROLLER

PARAMETER	VALUES
$k_p = V_o / (L * C)$	$1.16e^7 V / (rad/sec)^2$
$a_p = 1 / (R * C)$	135 (rad/sec)
$b_p = 1 / (L * C)$	$76e^3 (rad/sec)^2$
$\theta_1$	20
$\theta_2$	-0.783
$\theta_3$	$-2.25e^4$
$k_m$	$5.83 * 10^6 V / (rad/sec)^2$
$a_m$	$8.17 * 10^3 rad/sec$
$b_m$	$1.67 * 10^7 (rad/sec)^2$
$\lambda$	1
Transfer function of reference model	$1.1e^7 / s^2 + 135s + 85$

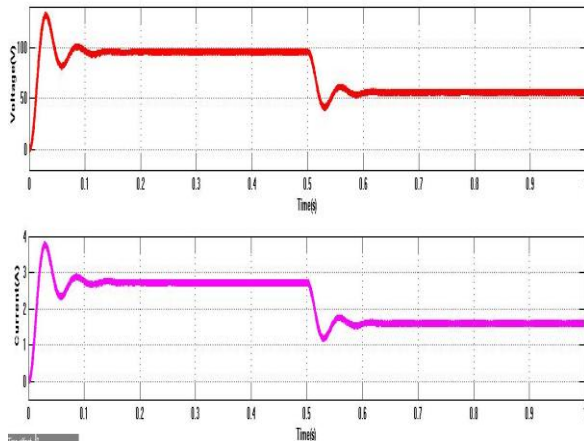


Fig.7 Array voltage and current obtained from overall proposed system.

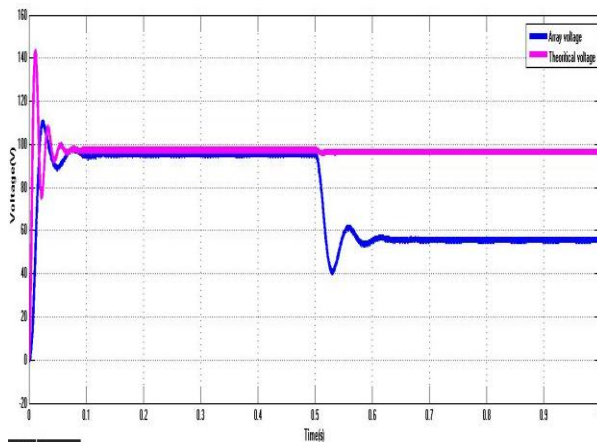


Fig 9: Adapted array voltage and theoretical MPP voltage

The array voltage and array current response is obtained for two different irradiance level shown in fig 7 .For the initial time the irradiance level is  $1000\text{W/m}^2$  and after 0.5 s irradiance level is  $500\text{ w/m}^2$  for the same temperature  $25^\circ$ .The array voltage converges to the nominal voltage at which maximum power can be obtained within the initial few seconds. Also the adapted array voltage shows no oscillatory response even after the first change in sunlight at 0.5s. Array voltage of the plant model for two different irradiance level is been simulated along with the reference model shown in fig 8 .Within the initial few seconds plant learns ,and the adapted array voltage dampens to the nominal voltage at the same time instant at which reference model dampens to its nominal voltage.From the comparison it is evident that plant model converges with the reference model with no oscillation and with the same rate of convergence .

## V. CONCLUSION

In order to improve the efficiency of photovoltaic systems, MPPT control algorithms are used to optimize the power output of the systems. The essential considerations are the

accuracy and convergence time. Here a two-level adaptive control architecture that can reduce complexity in system control and effectively handle the uncertainties and perturbations in the photovoltaic systems and the environment is proposed. The first level of control was RCC, and the second level was MRAC. As the simulation result extensively discussed in Section V, the statement that the proposed control system, by coupling two control algorithms, optimizes the performance of the solution to the maximum power point tracking is convincing

## REFERENCES

- [1] S. L. Brunton, C. W. Rowley, S. R.Kulkarni, and C. Clarkson, "Maximum power point tracking for photovoltaic optimization using ripple-based extremum seeking control," *IEEE Trans. Power Electron.*, vol. 25, no. 10,pp. 2531–2540, Oct. 2010.
- [2] R. A.Mastroauro,M. Liserre, T.Kerekes, and A Dell'Aquila, "A single phase voltage-controlled grid-connected photovoltaic system with power quality conditioner functionality," *IEEE Trans. Ind. Electron.*, vol. 56, no. 11, pp. 4436–4444, Nov. 2009.
- [3] A. K. Abdelsalam, A. M. Massoud, S. Ahmed, and P. N. Enjeti, "High-performance adaptive perturb and observe MPPT technique for photovoltaic-based microgrids," *IEEE Trans. Power Electron.*, vol. 26, no. 4, pp. 1010–1021, Apr. 2011.
- [4] M. A. Elgendy, B. Zahawi, and D. J. Atkinson, "Assessment of perturb and observe MPPT algorithm implementation techniques for PV pumping applications," *IEEE Trans. Sustainable Energy*, vol. 3, no. 1, pp. 21–33, Jan. 2012.
- [5] G. Petrone, G. Spagnuolo, and M. Vitelli, "A multivariable perturb-andobserve maximum power point tracking technique applied to a singlestage photovoltaic inverter," *IEEE Trans. Ind. Electron.*, vol. 58, no. 1, pp. 76–84, Jan. 2011.
- [6] JS. Jain andV.Agarwal, "A newalgorithm for rapid tracking of approximate maximum power point in photovoltaic systems," *IEEE Power Electron.Lett.*, vol. 2, no. 1, pp. 16–19, Mar. 2004.
- [7] N. Femia, G. Petrone, G. Spagnuolo, and M. Vitelli, "Optimization of perturb and observe maximum power point tracking method," *IEEE Trans.Power Electron.*, vol. 20, no. 4, pp. 963–973, Jul. 2005.
- [8] M. A. S. Masoum, H. Dehbonei, and E. F. Fuchs, "Theoretical and experimental analyses of photovoltaic systems with voltage and current-based maximum power-point tracking," *IEEE Trans. Energy Convers.*, vol. 17, no. 4, pp. 514–522, Dec. 2002.
- [9] T. Eswam and P. L. Chapman, "Comparison of photovoltaic array maximum power point tracking techniques," *IEEE Trans. Energy Convers.*, vol. 22, no. 2, pp. 439–449, Jun. 2007.
- [10] M. Veerachary, T. Senjyu, and K. Uezato, "Neural-network-based maximum-power-point tracking of coupled-inductor interleaved-boostconverter- supplied PV system using fuzzy controller," *IEEE Trans. Ind.Electron.*, vol. 50, no. 4, pp. 749–758, Aug. 2003.
- [11] P. T. Krein, "Ripple correlation control, with some applications," in *Proc. IEEE Int. Symp. Circuits Syst.*, 1999, vol. 5, pp. 283–286.
- [12] D. L. Logue and P. T. Krein, "Optimization of power electronic systems using ripple correlation control: A dynamic programming approach," in *Proc. IEEE 32nd Annu. Power Electron.Special. Conf.*, 2001, vol. 2, pp. 459–464.
- [13] J. W. Kimball and P. T. Krein, "Discrete-time ripple correlation control for maximum power point tracking," *IEEE Trans. Power Electron.*, vol. 23, no. 5, pp. 2353–2362, Sep. 2008.
- [14] T. Eswam, J. W. Kimball, P. T. Krein, P. L. Chapman, and P. Midya, "Dynamic maximum power point tracking of photovoltaic arrays using ripple correlation control," *IEEE Trans. Power Electron.*, vol. 21, no. 5, pp. 1282– 1291, Sep. 2006.
- [15] D. E. Miller, "A new approach to model reference adaptive control," *IEEE Trans. Autom. Control*, vol. 48, no. 5, pp. 743–757, May 2003.
- [16] S. Sastry and M. Bodson, *Adaptive Control: Stability, Convergence and Robustness*. New York: Dover Publications, 2011.